Inverse energy flux of focused radially polarized optical beams

S. N. Khonina,[1,2] A. V. Ustinov,[1] and S. A. Degtyarev[1,2]

[1]*Image Processing Systems Institute—Branch of the Federal Scientific Research Centre "Crystallography and Photonics" of Russian Academy of Sciences, 151 Molodogvardeyskaya Street, Samara 443001, Russia*

[2]*Samara National Research University, 34 Moskovskoye Shosse, Samara 443086, Russia*

(Received 18 July 2018; published 11 October 2018)

We report the formation of a negative energy flux in the case of tight focusing of an arbitrary-order radially polarized annular beam. We consider not only the longitudinal component of the Poynting vector (energy flux density) and the region of its negative values, but also the local inverse energy flux as an integral characteristic over the region of negative values. Theoretically, the Richards-Wolf formulas in the Debye approximation are used to maximize the negative value of the energy flux density on the optical axis in the focal region for the second-order radial polarization ($m = 2$). In this case, the local inverse energy flux, an integral characteristic in the bulk region of negative values, increases with increasing radial polarization order, i.e., for $m > 2$. Jones matrices are employed to show that the result obtained will be valid for azimuthal polarization, as well as for a circularly polarized vortex beam. The results of numerical simulation are in good agreement with theoretical calculations. In addition, taking into account the approximate nature of the Richards-Wolf formulas, we also additionally model the tight focusing of a circular beam based on the solution of Maxwell's equation using the finite element method. It is shown that the local inverse energy flux in the case of the second-order radial polarization will be 1.5 times less than that in the case of the third-order radial polarization. In turn, the use of the fourth-order radial polarization makes it possible to increase the local inverse energy flux by a factor of 2.

DOI: 10.1103/PhysRevA.98.043823

I. INTRODUCTION

Recently, the interest of researchers has focused on an inverse energy flux of nonparaxial laser beams, namely, the negative values of the Poynting vector in the local domain.

The authors of Ref. [1] considered the energy characteristics of the superposition of TE- and TM-polarized Bessel beams. The expression obtained for the Poynting vector shows that under certain conditions, both the longitudinal and azimuthal components can change their sign. Negative values of the azimuthal component mean that the angular momentum is directed opposite to that in the neighboring regions. The negative longitudinal component corresponds to a more interesting physical phenomenon, i.e., propagation of the beam in the opposite direction with respect to the optical axis. Similar opposite directions of vectors are observed in a medium with a negative dielectric permittivity and magnetic permeability [2,3]. It was shown [1] that the longitudinal component of the Poynting vector assumes the largest negative value on the optical axis in the case of circular polarization. The modulus of the negative minimum of the longitudinal component does not exceed 25%–30% of the positive maximum. We believe that this ratio can be increased by using a different beam type.

Monteiro *et al.* [4] investigated in detail the tight focusing of circularly polarized Laguerre-Gaussian beams with orbital indices $(0, l)$ (where l is the order of the optical vortex). Analytical expressions were obtained for the electric field components, the Poynting vector, the angular momentum density, and the angular momentum flux density. Among various effects, the authors of Ref. [4] found that in the nonparaxial regime, due to the interaction between the phase vortex singularity (at $|l| \geqslant 2$) and the spin angular momentum, the energy propagates in the direction opposite to that of the incident beam near the optical axis. However, judging from the figures in Ref. [4] we may conclude that the value of the negative minimum modulus of the longitudinal component of the Poynting vector does not exceed 12% of the positive maximum.

One more type of beam, i.e., the Airy beam, was considered in [5]. The propagation of nonparaxial Airy beams was described theoretically on the basis of the angular spectrum of the incident beam with the separate contributions of propagating and evanescent waves. In this case, the longitudinal component of the Poynting vector is represented as the sum of three terms: the contribution of propagating waves, evanescent waves, and the interference term. Negative values of the longitudinal component of the Poynting vector, corresponding to the energy backpropagation, appear only with a large degree of nonparaxiality. It was theoretically proved that negative values are achieved due to the term corresponding to the interaction of propagating and evanescent waves. In this case, the inverse energy flux of the Airy beams is observed separately in the TE or TM mode, rather than in a complex superposition as in the case of Bessel beams [1]. Note, however, that for Airy beams, the value of the negative energy flux density is only 11% of the positive maximum.

Mitri [6] presented analytical expressions for the components of the electromagnetic field of nonparaxial vortex Bessel beams with a fractional topological charge. These expressions were used to obtain conditions under which the values of the longitudinal component of the Poynting vector are negative. The best conditions included significant nonparaxiality, a topological charge equal to 2, and circular polarization.

Recently, the idea of combining the vortex beams with circular polarization of opposite sign, initially suggested in

[4] for the Laguerre-Gaussian beams, was generalized for an arbitrary circularly polarized optical vortex with an integer topological charge m in [7]. Kotlyar *et al.* [7], using the Richards-Wolf (RW) formulas, showed that, regardless of the beam amplitude and the apodization function, negative values for the energy flux density are observed near the optical axis. For $m = 2$, the maximum relative value of the negative value of the energy flux density of about 0.8 was obtained. At $m = 3$, this value decreases to about 0.35.

Thus, based on the above review, it follows that the maximum value of the negative energy flux density is attained for the vortex phase singularity $m = 2$ in the case of circular polarization of the opposite direction. However, if we consider not the maximum value, but the entire range of negative values, then other types of beams may suit better.

In this paper, we consider the formation of a negative energy flux in the case of tight focusing of an arbitrary-order radially polarized annular beam. Theoretically, using the RW formulas, the negative value of the energy flux density on the optical axis in the focal region for the second-order radial polarization is maximized. In this case, the local inverse energy flux as an integral characteristic in the bulk region of negative values increases with increasing order of the radial polarization. The validity of theoretical calculations is further justified by numerical calculations both using the RW formulas and in the framework of a rigorous electromagnetic theory.

The presence of an inverse energy flux extends the capabilities of optical trapping and manipulation. The action on the particles in this case will be similar to "tractor beams" [8–11], meaning that the light does not push the particles forward in the direction of propagation, but pulls it back. Furthermore, the presence of an inverse energy flux is useful in the detection of invisibility cloaks [12,13] and other applications.

II. THEORETICAL ANALYSIS FOR THE TIGHT FOCUSING OF A CIRCULAR BEAM IN THE DEBYE APPROXIMATION

The vectors of the electric and magnetic fields in the focal region in the Debye approximation are determined by the RW formulas [14–17]:

$$\begin{bmatrix}\mathbf{E}(r,\varphi,z)\\ \mathbf{H}(r,\varphi,z)\end{bmatrix} = -\frac{if}{\lambda}\int_0^{\alpha}\int_0^{2\pi} T(\theta)F(\theta,\phi)\begin{bmatrix}\mathbf{P}_E(\theta,\phi)\\ \mathbf{P}_H(\theta,\phi)\end{bmatrix} \times \exp\left(ik[r\sin\theta\cos(\phi-\varphi)+z\cos\theta]\right) \times \sin\theta d\theta d\phi, \quad (1)$$

where

$$\mathbf{P}_E(\theta,\phi) = \begin{bmatrix} A(\theta,\phi) & C(\theta,\phi)\\ C(\theta,\phi) & B(\theta,\phi)\\ -D(\theta,\phi) & -E(\theta,\phi)\end{bmatrix}\begin{bmatrix}c_x(\phi)\\ c_y(\phi)\end{bmatrix},$$

$$\mathbf{P}_H(\theta,\phi) = \begin{bmatrix} C(\theta,\phi) & -A(\theta,\phi)\\ B(\theta,\phi) & -C(\theta,\phi)\\ -E(\theta,\phi) & D(\theta,\phi)\end{bmatrix}\begin{bmatrix}c_x(\phi)\\ c_y(\phi)\end{bmatrix}, \quad (2)$$

$$\begin{aligned} A(\theta,\phi) &= 1+\cos^2\phi(\cos\theta-1),\\ B(\theta,\phi) &= 1+\sin^2\phi(\cos\theta-1),\\ C(\theta,\phi) &= \sin\phi\cos\phi(\cos\theta-1),\\ D(\theta,\phi) &= \cos\phi\sin\theta,\\ E(\theta,\phi) &= \sin\phi\sin\theta, \end{aligned} \quad (3)$$

where $F(\theta,\phi)$ is the amplitude of the initial field; $\left[\begin{smallmatrix}c_x(\phi)\\ c_y(\phi)\end{smallmatrix}\right]$ is the vector of the polarization coefficients, whose norm is equal to unity; and $T(\theta)$ is the apodization function [for an aplanatic lens $T(\theta) = \sqrt{\cos\theta}$].

Consider the situation where the amplitude of the initial field $F(\theta,\phi)$ is concentrated in a narrow annular region with a central angle θ_0 and width $\Delta\theta$:

$$F(\theta,\phi) = \begin{cases} F_0(\phi), & \theta_0-\Delta\theta/2 \leqslant \theta \leqslant \theta_0+\Delta\theta/2,\\ 0, & \text{else.}\end{cases} \quad (4)$$

Note that the concentration of energy in a narrow annular region does not always mean a small amount of energy (as occurs when an annular gap is used [18]). In particular, a ring with a high energy content can be formed with the help of an axicon in the focal plane of the lens [19].

Let us find out analytically for field (4), in which for cases under conditions of tight focusing [when formulas (1)–(3) are applicable], it is possible to have regions with an inverse energy flux, and in general, attention will be paid to situations where one of these regions is near the optical axis.

By the definition, the time-averaged energy flux density (Poynting vector) is [20]

$$\mathbf{S} = \frac{c}{8\pi}\mathrm{Re}(\mathbf{E}\times\mathbf{H}^*) = \frac{c}{8\pi}\mathrm{Re}(\mathbf{E}^*\times\mathbf{H}). \quad (5)$$

The longitudinal component of the vector $\mathbf{S}$ is accurate to a constant coefficient and equals

$$S_z = \mathrm{Re}(E_x^*H_y - E_y^*H_x). \quad (6)$$

For an input field of form (4), the components of the focused electromagnetic field in (1), participating in (6), will be calculated by the formulas

$$\begin{aligned} E_x^*(r,\varphi,z) &\approx p(-z)\int_0^{2\pi} F_0^*(\phi)[A(\theta_0,\phi)c_x^*(\phi)+C(\theta_0,\phi)c_y^*(\phi)]\exp[-ikr\sin\theta_0\cos(\phi-\varphi)]d\phi,\\ E_y^*(r,\varphi,z) &\approx p(-z)\int_0^{2\pi} F_0^*(\phi)[C(\theta_0,\phi)c_x^*(\phi)+B(\theta_0,\phi)c_y^*(\phi)]\exp[-ikr\sin\theta_0\cos(\phi-\varphi)]d\phi,\\ H_x(r,\varphi,z) &\approx p(z)\int_0^{2\pi} F(\phi)[C(\theta_0,\phi)c_x(\phi)-A(\theta_0,\phi)c_y(\phi)]\exp[ikr\sin\theta_0\cos(\phi-\varphi)]d\phi,\\ H_y(r,\varphi,z) &\approx p(z)\int_0^{2\pi} F(\phi)[B(\theta_0,\phi)c_x(\phi)-C(\theta_0,\phi)c_y(\phi)]\exp[ikr\sin\theta_0\cos(\phi-\varphi)]d\phi, \end{aligned} \quad (7)$$

where $p(z) = -if\Delta\theta T(\theta_0)\exp(ikz\cos\theta_0)\sin\theta_0/\lambda$.

Note that for axisymmetric beams, for which $F(\phi) = const.$, the integrals in expressions (7) are computed explicitly. This is also valid for some other beams, including vortices; i.e., $F(\phi) = \exp(im\phi)$.

Next, we consider various variants of the polarization state and the vortex phase singularity for the circular field (7), which ensure the presence of negative values of the longitudinal projection of the Poynting vector (6), i.e., presence of a negative energy flux density.

A. Radial polarization of arbitrary order in the absence of a vortex phase singularity

This polarization state is considered in order to form a negative energy flux in the case of tight focusing of an annular beam. The radially polarized light is ensuring the sharpest focus, i.e., the minimal focal spot size [15–18,21,22]. In the case of the radial polarization of arbitrary order m [23,24] $F(\theta_0, \phi) \equiv 1$, $c_x(\phi) = \cos(m\phi)$, and $c_y(\phi) = \sin(m\phi)$ (the value $m = 0$ corresponds to the linear x polarization).

The components of field (7) participating in expression (6) can be calculated analytically using trigonometric formulas and tabulated integrals ([25], p. 456):

$$\int_{-\pi}^{\pi} \exp(iz\cos x)\cos(nx)dx = 2\pi i^n J_n(z),$$
$$\int_{-\pi}^{\pi} \exp(iz\cos x)\sin(nx)dx = 0. \tag{8}$$

Without going into the details of the intermediate calculations, we give the resulting expression:

$$S_z(r) = (\Delta\theta)^2 T^2(\theta_0)\sin^2\theta_0\pi^2 \times [(1+\cos\theta_0)^2 J_m^2(t) - (1-\cos\theta_0)^2 J_{m-2}^2(t)], \quad t = kr\sin\theta_0. \tag{9}$$

Expression (9) has an explicit form without integrals and allows one to analyze the properties of the energy flux-density function.

It is obvious that the direction of the energy flux density is determined by the sign of the expression in square brackets in (9), so it is sufficient to consider only that. Since the equality $J_{-n}(t) = (-1)^n J_n(z)$, $n > 0$ holds, there are three essentially different cases: $m \leqslant 0$, $m = 1$, and $m \geqslant 2$.

1. Case 1: $m < 0$

In this case we obtain from (9)

$$S_z \sim (1+\cos\theta_0)^2 J_{|m|}^2(t) - (1-\cos\theta_0)^2 J_{|m|+2}^2(t). \tag{10}$$

Since, for small values of the argument, the Bessel function decreases with increasing order (especially with allowance for the fact that the coefficient for a function of smaller order is larger), then, obviously, expression (10) near the optical axis will be positive. There exist regions of negative values of S_z in (10): these are rings with a width decreasing with distance from the optical axis. To assess the effectiveness of achieving the formulated goal, we introduce a characteristic that is the ratio of the negative minimum to the positive maximum:

$$\eta = \frac{|\min S_z|}{\max S_z}. \tag{11}$$

In the case under study, η increases with increasing $|m|$ and at $\theta_0 \to 90^\circ$. However, we can prove that there will always be $\eta < 1$. For us this case is off interest.

2. Case 2: $m = 1$

In this case,

$$S_z \sim 4\cos\theta_0 J_1^2(t); \tag{12}$$

i.e., the energy flux density is always positive, which means that in the case of standard radial polarization (first order), the inverse energy flux cannot be observed.

3. Case 3: $m \geqslant 2$

In this case,

$$S_z \sim (1+\cos\theta_0)^2 J_m^2(t) - (1-\cos\theta_0)^2 J_{m-2}^2(t). \tag{13}$$

At small values of the argument, the Bessel function decreases with increasing order; therefore, despite the fact that the coefficient for the function of higher order is larger, expression (13) near the optical axis will be negative. Note that the region of negative values S_z is not limited to the central part; it also includes rings with a width that decreases with distance from the optical axis. However, the highest values of η will be achieved in the central part at $m = 2$ on the optical axis.

Since the maximum values of the Bessel function decrease with increasing order, the largest value of η should be reached at $m = 2$. Let us consider this case in more detail:

$$S_z \sim (1+\cos\theta_0)^2 J_2^2(t) - (1-\cos\theta_0)^2 J_0^2(t). \tag{14}$$

Obviously, a negative minimum is reached at $t = 0$. Finding a positive maximum is not so trivial, since the maximum of the first summand and the minimum of the second one are attained for different values of the argument. After a detailed analysis, we arrive at the expression

$$\eta = \begin{cases} \frac{(1-\cos\theta_0)^2}{0.236(1+\cos\theta_0)^2 - 0.076(1-\cos\theta_0)^2} = \left[0.236\left(\frac{1+\cos\theta_0}{1-\cos\theta_0}\right)^2 - 0.076\right]^{-1}, & 0 \leqslant \theta_0 < 84^\circ, \\ \frac{(1-\cos\theta_0)^2}{0.186(1+\cos\theta_0)^2} = 5.376\left(\frac{1-\cos\theta_0}{1+\cos\theta_0}\right)^2, & 84^\circ \leqslant \theta_0 \leqslant 90^\circ. \end{cases} \tag{15}$$

Analysis of expression (15) shows that the maximum value of $\eta = 5.376$ is achieved in the case of the tightest focusing, i.e., at $\theta_0 = 90^\circ$. As the angle θ_0 decreases, the value of the inverse energy flux density decreases. In particular, $\eta = 3.541$ for $\theta_0 = 84^\circ$, $\eta = 1$ for $\theta_0 = 68^\circ 46'$, and $\eta \underset{\theta_0 \to 0}{\to} 0$.

Thus, it is shown that a much larger relative value (by more than five times) of the inverse energy flux density can be achieved in comparison with the results obtained previously in other studies.

Note that if we consider absolute values rather than relative ones, then due to apodization $T(\theta) = \sqrt{\cos\theta}$ in the aplanatic lens model, the maximum value of the inverse energy flux density will be achieved at a smaller angle. If we take into account all factors in formula (9), the maximum value of the inverse energy flux density will be at the angle $\theta_0 = \arccos[(\sqrt{24}-2)/10] \approx 73^\circ$ (in this case, $\eta = 1.423$).

Next we will pay attention to another important issue. As a rule, most publications consider only the energy flux density; however, for different applications, especially in the case of optical trapping and manipulation, the total energy flux as an integral characteristic plays an important role. Note that to act on a small particle, one needs a local energy flux over a region Ω of negative values:

$$\hat{S} = \int_{\Omega} S_z d\Omega. \tag{16}$$

To estimate the local negative energy flux (16), we define the region Ω of negative values in the focal plane.

For positive m, the radius r_{neg} of a circle with an inverse energy flux can be obtained from the following equation (taking its smallest positive root):

$$(1+\cos\theta_0)^2 J_m^2(k\sin\theta_0 r_{\text{neg}}) = (1-\cos\theta_0)^2 J_{m-2}^2(k\sin\theta_0 r_{\text{neg}}). \tag{17}$$

While this equation does not have an explicit solution, it can be shown that the value of r_{neg} decreases with decreasing θ_0. The largest value of r_{neg} will be reached at $\theta_0 \to 90^\circ$, and it can be found analytically:

$$r_{\text{neg}} = j'_{m-1,1}/k, \tag{18}$$

where $j'_{m,1}$ is the first root of the derivative of the mth-order Bessel function

In particular, for $m = 2$, $r_{\text{neg}} \approx 1.84/k \approx 0.293\lambda$, and for $m = 3$, $r_{\text{neg}} \approx 0.485\lambda$. The radius of the region of negative values (18) increases with increasing m approximately linearly. This is important for optical manipulation of microparticles because the size of the region of influence on the particle must be comparable with the particle size.

Taking into account the calculated radius of the region of negative values, we can calculate the local inverse energy flux as follows:

$$\hat{S} = \int_0^{r_{\text{neg}}} S_z(r) r dr. \tag{19}$$

For $m > 2$, the largest negative values of S_z will be achieved on some circle near the optical axis (on the optical axis $S_z = 0$). In this case, the values of η will be smaller than for $m = 2$, but the domain Ω of negative values will be larger. Consequently, one can expect an increase in the local negative energy flux $\hat{S}$. For the limiting angle $\theta_0 \to 90^\circ$, it can theoretically be shown that $\hat{S} \sim \sqrt[3]{m-1}$.

B. Other types of the polarization state

For the longitudinal component of the Poynting vector (6), the distribution of the transverse electromagnetic-field components is important. Let us evaluate the potentialities of other types of the polarization state on the basis of their representation through the Jones matrices. In particular, the above-considered radial polarization of the mth order can be represented through a superposition of circularly polarized vortex fields:

$$\begin{aligned}\begin{pmatrix} E_x \\ E_y \end{pmatrix} &= F(\theta,\phi)\begin{bmatrix} \cos(m\phi) \\ \sin(m\phi) \end{bmatrix} \\ &= \frac{1}{2}F(\theta,\phi)\begin{bmatrix} \exp(im\phi)+\exp(-im\phi) \\ -i\exp(im\phi)+i\exp(-im\phi) \end{bmatrix} \\ &= \frac{1}{2}F(\theta,\phi)\left[\exp(im\phi)\begin{pmatrix} 1 \\ -i \end{pmatrix} + \exp(-im\phi)\begin{pmatrix} 1 \\ i \end{pmatrix}\right].\end{aligned} \tag{20}$$

It follows from expression (20) that for circular polarization with a vortex phase of the mth order one can obtain results analogous to those obtained in the previous section.

Obviously, the same result will be for the azimuthal polarization of the mth order:

$$\begin{aligned}&F(\theta,\phi)\begin{bmatrix} -\sin(m\phi) \\ \cos(m\phi) \end{bmatrix} \\ &= \frac{1}{2}F(\theta,\phi)\begin{bmatrix} i\exp(im\phi)-i\exp(-im\phi) \\ \exp(im\phi)+\exp(-im\phi) \end{bmatrix} \\ &= \frac{1}{2}F(\theta,\phi)\left[-\exp(im\phi)\begin{pmatrix} 1 \\ -i \end{pmatrix} + \exp(-im\phi)\begin{pmatrix} 1 \\ i \end{pmatrix}\right].\end{aligned} \tag{21}$$

Thus, we have obtained a generalization of the well-known optimal result for circular polarization with a second-order vortex phase. Taking into account the analysis carried out in Sec. II A, circular polarization with a vortex phase of higher orders, as well as azimuthal polarization of high orders, will potentially allow a larger local negative energy flux $\hat{S}$.

III. NUMERICAL CALCULATION FOR TIGHT FOCUSING OF A CIRCULAR BEAM IN THE DEBYE APPROXIMATION

This section presents the calculation results for the longitudinal component of the Poynting vector (6) using expressions (1)–(3) for the distribution (4) at $\theta_0 = 80^\circ$, $\Delta\theta = 3^\circ$ with arbitrary-order radial polarization. Figures 1 and 2 show, respectively, the results for the first (at $m < 0$) and third (at $m \geqslant 2$) cases considered in Sec. II A. The positive part of S_z is shown in blue, and the negative part in red.

As can be seen from the results shown in Figs. 1 and 2, the numerical simulation completely agrees with the theoretical calculations of Sec. II. In all cases (except $m = 1$), radial polarization allows negative values to be obtained. However, at $m \geqslant 2$ the inverse energy flux density is concentrated near the optical axis, which is of greatest interest for optical manipulation.

Table I lists the calculated characteristics of the ratio of the negative minimum to the positive maximum η (11) and the local energy flux in the region of negative $\hat{S}$ (19).

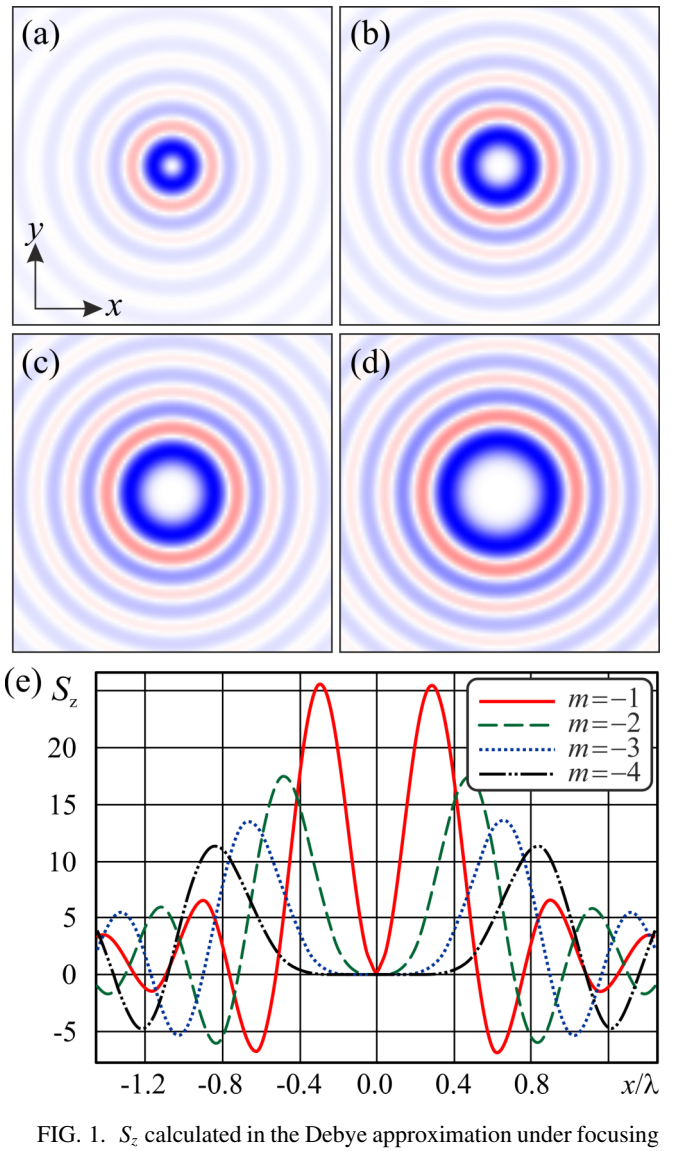

FIG. 1. S_z calculated in the Debye approximation under focusing a radially polarized circular field at $m < 0$: (a) $m = -1$, (b) $m = -2$, (c) $m = -3$, (d) $m = -4$; panel (e) shows the normalized cross sections along the X axis. In panels (a) through (e), x and y range from $-2.5\,\lambda$ to $+2.5\,\lambda$.

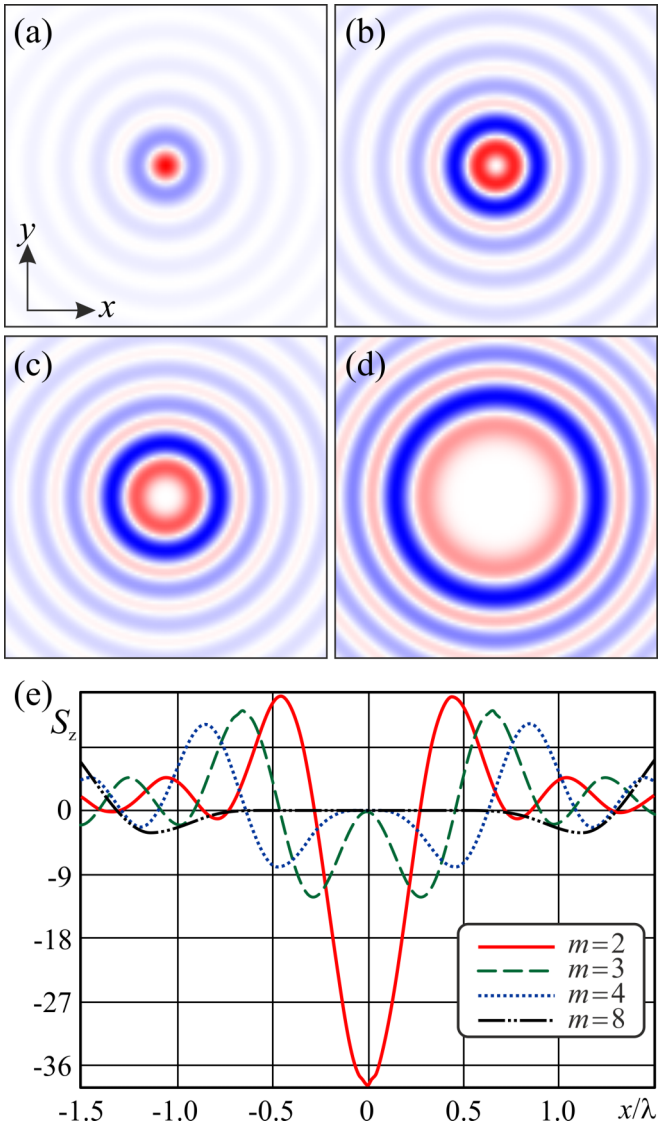

FIG. 2. S_z calculated in the Debye approximation under focusing a radially polarized circular field at $m \geqslant 2$: (a) $m = 2$, (b) $m = 3$, (c) $m = 4$, (d) $m = 8$; panel (e) shows the normalized cross sections along the X axis. In panels (a) through (e), x and y range from $-2.5\,\lambda$ to $+2.5\,\lambda$.

The results given in Table I confirm the effect predicted in Sec. II: Although a relatively large minimum ($\eta = 2.39$) is reached at $m = 2$, the local inverse energy flux increases with increasing m. The $\hat{S}$ increases nonlinearly (as predicted in Sec. II A); i.e., a higher rate of change occurs for small values of m.

TABLE I. Calculated characteristics of η and $\hat{S}$ for radial polarization of mth order.

m	**2**	**3**	**4**	**8**
η	2.39	0.87	0.65	0.4
r_{neg}	0.27λ	0.46λ	0.63λ	1.31λ
$\hat{S}$ (Normalized)	1	1.3	1.49	1.83

The results of numerical simulation for azimuthal polarization and circularly polarized vortex beams coincide with the results presented for radial polarization, which agrees with the calculations in Sec. II B.

It should be noted that the results of Secs. II and III were obtained within the framework of the approximate Debye model [15]. The conditions for the applicability of this model include the following: linear dimensions of the exit pupil are large compared with the wavelength [14], and the focal point is placed many wavelengths away from the aperture [15]. Thus, the Debye approximation does not guarantee the correctness of the results for the elements of micro-optics. Therefore, to confirm the results obtained on the scale of micro-optics, it is necessary to calculate the electric and magnetic fields by directly solving Maxwell's equations.

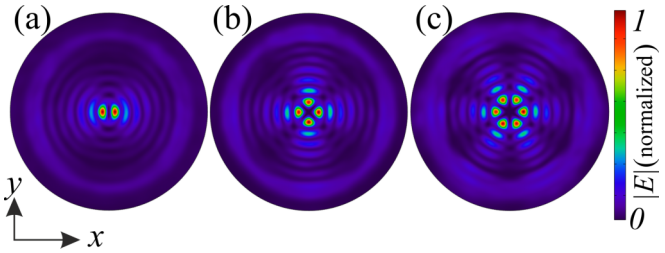

FIG. 3. Square of the electric field amplitude calculated by the finite element method under the focusing of a radially polarized annular field at $m \geqslant 2$: (a) $m = 2$, (b) $m = 3$, (c) $m = 4$. x and y range from $-5\,\lambda$ to $+5\,\lambda$.

IV. NUMERICAL CALCULATION FOR TIGHT FOCUSING OF A CIRCULAR BEAM BY THE FINITE ELEMENT METHOD

In this section, based on the finite element method implemented in the COMSOL software package we calculate the focusing of a plane wave limited by a ring aperture. The calculated region has the form of a cylinder of length 7λ and radius of 5.2λ.

The amplitude distribution in the $z = 0$ plane has the form

$$E_x = \exp\left[-\frac{ik(x^2+y^2)}{2f}\right]\cos(m\varphi)\mathrm{ring}(\sqrt{x^2+y^2}),$$
$$E_y = \exp\left[-\frac{ik(x^2+y^2)}{2f}\right]\sin(m\varphi)\mathrm{ring}(\sqrt{x^2+y^2}). \quad (22)$$

The focusing phase is given by a factor $\exp[-\frac{ik(x^2+y^2)}{2f}]$. Here, f is the focal length equal to λ, and the ring aperture with an internal radius 4λ and outer radius 5λ is determined by the factor $\mathrm{ring}(\sqrt{x^2+y^2})$:

$$\mathrm{ring}(r) = \begin{cases} 1, & 4\lambda < r < 5\lambda, \\ 0, & \text{else}. \end{cases} \quad (23)$$

The distributions of the electric field amplitudes are shown in Fig. 3.

Figure 4 shows the distribution of the longitudinal component of the power flux density vector in the transverse cross section of a beam with radial polarization of different orders.

One can see from comparing Figs. 2 and 4 that the radial symmetry of the solution is violated when solving the Maxwell equations.

Based on the simulation performed, we have obtained the results similar to those in the fourth row of Table I. The integral value of the inverse flux $\hat{S}$ is calculated in a tube of radius 0.7λ, with the axis of the tube coinciding with the optical axis of the focused beam. The length of the tube is 10λ and constitutes the entire modeling area. The calculations have shown that for $m = 3$ the integral value of the inverse flux is 1.5 times larger than for $m = 2$, and for $m = 4$ it is almost two times larger than for $m = 2$.

On the basis of the results of this section, we can conclude that the Debye approximation gives similar results for the values of integral fluxes, but it does not take into account the loss of symmetry of the spatial field distribution.

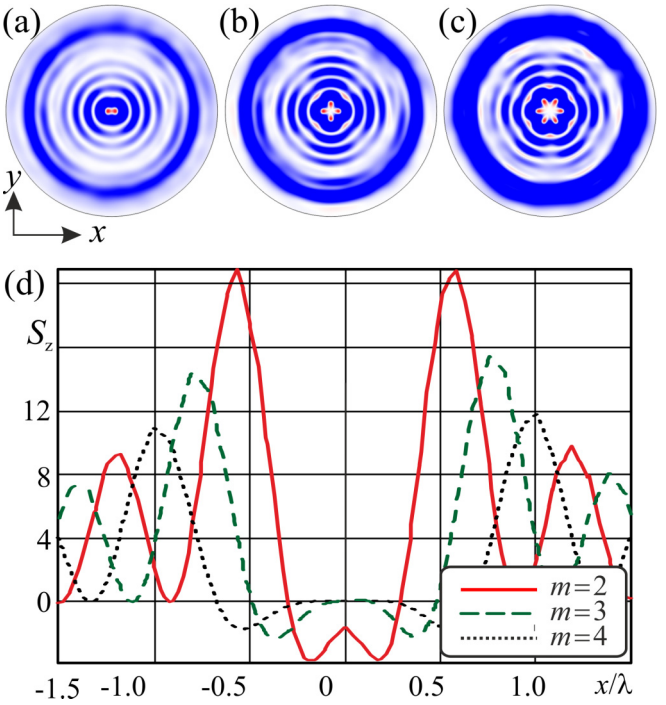

FIG. 4. S_z calculated by the finite element method under the focusing of a radially polarized circular field at $m \geqslant 2$: (a) $m = 2$, (b) $m = 3$, (c) $m = 4$; panel (d) shows the normalized cross sections along the X axis. In panels (a) through (c), x and y range from $-5\,\lambda$ to $+5\,\lambda$.

V. CONCLUSIONS

We have considered the appearance of an inverse energy flux in a tightly focused circular beam with radial polarization of arbitrary order. The following results have been obtained:

(1) In the Debye approximation, explicit formulas for the energy flux density in the focal plane have been derived as a function of radius. These formulas allow one to obtain quantitative characteristics of the longitudinal projection of the Poynting vector (zero-crossing positions, minimum and maximum values in each of the constant-sign regions).

(2) Analysis of theoretical expressions has shown that the maximization of the negative value of the energy flux density on the optical axis will occur in the case of second-order radial polarization ($m = 2$). In this case, the Debye model predicts a much larger relative value (by more than five times) of the inverse energy flux density in comparison with the results obtained previously in other papers.

(3) The local inverse energy flux as an integral characteristic over a region of negative values has been shown theoretically and numerically to increase with increasing order of radial or azimuthal polarization or with increasing order of the vortex singularity for circular polarization. This effect is associated with an increase in the range of negative values with increasing number m. The result obtained is important for the optical manipulation of microparticles, because the size of the region of influence on the particle must be comparable with the particle size.

(4) On the basis of Jones matrices, it has been shown that the result obtained for radial polarization will be valid for

azimuthal polarization, as well as for a circularly polarized vortex beam.

(5) Numerically, using the finite element method, it has been shown that the local inverse energy flux in the case of tight focusing of a radially polarized beam will increase with increasing polarization order.

The obtained results are important in extending the capabilities of optical trapping and manipulation.

ACKNOWLEDGMENTS

This work was financially supported by the Russian Foundation for Basic Research (Grant No. 16-29-11698-ofi_m) for part of the theoretical investigations and by the Ministry of Science and Higher Education within the State assignment FSRC "Crystallography and Photonics" RAS (Agreement No. 007-GZ/C3363/26) for part of the numerical calculations.

[1] A. V. Novitsky and D. V. Novitsky, Negative propagation of vector Bessel beams, J. Opt. Soc. Am. A **24**, 2844 (2007).

[2] D. Schurig and D. R. Smith, Negative index lens aberrations, Phys. Rev. E **70**, 065601(R) (2004).

[3] A. Salandrino and D. N. Christodoulides, Reverse optical forces in negative index dielectric waveguide arrays, Opt. Lett. **36**, 3103 (2011).

[4] P. B. Monteiro, P. A. M. Neto, and H. M. Nussenzveig, Angular momentum of focused beams: Beyond the paraxial approximation, Phys. Rev. A **79**, 033830 (2009).

[5] P. Vaveliuk and O. Martinez-Matos, Negative propagation effect in nonparaxial Airy beams, Opt. Express **20**, 26913 (2012).

[6] F. G. Mitri, Reverse propagation and negative angular momentum density flux of an optical nondiffracting nonparaxial fractional Bessel vortex beam of progressive waves, J. Opt. Soc. Am. A **33**, 1661 (2016).

[7] V. V. Kotlyar, A. A. Kovalev, and A. G. Nalimov, Energy density and energy flux in the focus of an optical vortex: Reverse flux of light energy, Opt. Lett. **43**, 2921 (2018).

[8] S. Sukhov and A. Dogariu, On the concept of "tractor beams", Opt. Lett. **35**, 3847 (2010).

[9] A. Novitsky, C.-W. Qiu, and H. Wang, Single Gradientless Light Beam Drags Particles as Tractor Beams, Phys. Rev. Lett. **107**, 203601 (2011).

[10] S. Sukhov and A. Dogariu, Negative Nonconservative Forces: Optical "Tractor Beams" for Arbitrary Objects, Phys. Rev. Lett. **107**, 203602 (2011).

[11] J. J. Saenz, Laser tractor beams, Nat. Photonics **5**, 514 (2011).

[12] B. Zhang and B. I. Wu, Electromagnetic Detection of a Perfect Invisibility Cloak, Phys. Rev. Lett. **103**, 243901 (2009).

[13] C. Lan, Y. Yang, Z. Geng, B. Li, and J. Zhou, Electrostatic field invisibility cloak, Sci. Rep. **5**, 16416 (2015).

[14] B. Richards and E. Wolf, Electromagnetic diffraction in optical sysems. II. Structure of the aplanatic system, Proc. R. Soc. London **253**, 358 (1959).

[15] L.E. Helseth, Optical vortices in focal regions, Opt. Commun. **229**, 85 (2004).

[16] S. F. Pereira and A. S. van de Nes, Superresolution by means of polarisation, phase and amplitude pupil masks, Opt. Commun. **234**, 119 (2004).

[17] S. N. Khonina, Simple phase optical elements for narrowing of a focal spot in high-numerical-aperture conditions, Opt. Eng. **52**, 091711 (2013).

[18] R. Dorn, S. Quabis, and G. Leuchs, Sharper Focus for a Radially Polarized Light Beam, Phys. Rev. Lett. **91**, 233901 (2003).

[19] S. N. Khonina, Simple way for effective formation of various nondiffractive laser beams, Comput. Opt. **33**, 70 (2009).

[20] J. D. Jackson, *Classical Electrodynamics*, 3rd ed. (Wiley, New York, 1999).

[21] Y. Kozawa and S. Sato, Sharper focal spot formed by higher-order radially polarized laser beams, J. Opt. Soc. Am. A **24**, 1793 (2007).

[22] G. M. Lerman and U. Levy, Effect of radial polarization and apodization on spot size under tight focusing conditions, Opt. Express **16**, 4567 (2008).

[23] M. Stalder and M. Schadt, Linearly polarized light with axial symmetry generated by liquid-crystal polarization converters, Opt. Lett. **21**, 1948 (1996).

[24] C. X. Weng, L. Du, Z. Yang, C. Min, and X. Yuan, Generating arbitrary order cylindrical vector beams with inherent transform mechanism, IEEE Photonics J. **9**, 6100208 (2017).

[25] A. P. Prudnikov, Yu. A. Brychkov, and O. I. Marichev, *Integrals and Series* (Gordon and Breach Science Publishers, Amsterdam, 1983), Volume 1: Elementary Functions.